Study on Electromagnetic Interference of High-Speed Railway EMU

Liu Jin-Jiang, Cheng Qiang, Cheng Ning
Nanyang Normal University, Nanyang 473061, China
e-mail:chess12@126.com

Abstract

Electromagnetic radiation generated by pantograph-catenaries detachment is one of the inevitable problems with the development of high-speed railway this paper is focusing on the generating mechanism and characteristics of electromagnetic noise caused by pantograph-catenaries system. Based on previous research, we build an integrated model of catenaries and locomotive system, and study the electromagnetic disturbance characteristics using software FEKO. The simulation experiment results in the end can not only provide accurate data, but also give a more intuitive understanding of electromagnetic field distribution and attenuation characteristics generated by pantograph detachment.

Keywords: pantograph-catenaries detachment; high-speed railway; electromagnetic radiation

1. Introduction

In China, high-speed EMU run on speed of 200 ~ 250 km / h, power supplied by the 25 kV 50 Hz(AC). There is not only frequency electric field generated by catenaries at the top of compartment, but also high-frequency electromagnetic radiation caused by mounted motor, transformers and other equipments in the bottom. Whereas the pantograph system is the main harassment sources of train electromagnetic interference, especially when the pantograph spark occurs, it will seriously affect the locomotive communication, and even threaten the vehicles driving safety [1-5].

Electric arc generated by catenaries system is a big problem in high-speed EMU system, it is an air discharge phenomenon, when pantograph high-speed sliding on the electric line in tangential direction, with a relatively slow sliding at a small range of normal direction. High frequency components of catenaries arc spectrum are mainly distributed in 3 ~ 50 MHz, and emit high frequency noise to interference the communication signals and radio signals around locomotive, and even cause breakdown or distortion to communication and radio signals, what's more, high-frequency noise will affect vehicle communications, so it is a hazard of safe diving. In this paper, with electromagnetic simulation software we simulate the actual train environment; complete a targeted research on pantograph electromagnetic radiation

2. Electromagnetic Radiation Caused by Pantograph Disconnection
2.1. Gas Discharge Process

The basic process of gas discharge is: excitation, ionization, deionization, migration, proliferation. The mutual constraints of basic process determine the specific form and character of the discharge. Under normal circumstances, the pantograph have a good contact with contact line, locomotives thereby obtain energy from the grid so that EMU get high-speed, while the pantograph detachment of occurs, due to the voltage increases rapidly, reaching the gas breakdown point, start spark discharge, temperature rise sharply, releasing energy in the form of arc, and constitutes a complex electromagnetic environment generated by arc high-frequency electromagnetic radiation, affecting factors involves the amount of energy ,the generation and extinguish mechanism of arc, temporal and spatial distribution, energy transmission characteristics and other aspects. Therefore, it is necessary to study their theoretical analysis and experimental simulation method. The spectrum of electromagnetic pulses noise generated by pantograph system covers from tens kHz to GHz [6-9].

2.2. Field Strength Calculation of Electromagnetic Waves Spreading

Assuming wave source at point O, and wave source radiate energy uniformly, radiated power is P_Σ, the energy density at distance d from the wave source is

$$S = \frac{P_\Sigma}{4\pi d^2} \tag{1}$$

When distance d meet far field conditions, the electromagnetic wave can be considered as a uniform plane wave, such that the phase angle of electric and magnetic fields are all the same, but the ratio of electric field strength (E_0) and magnetic field strength (H_0) $E_0 / H_0 = 120\pi\Omega$, thus the average power of per unit area is

$$S = E_0 H_0 = \frac{E_0^2}{120\pi} \tag{2}$$

By formula (1) (2), we can obtain

$$E_0 = \frac{\sqrt{30\,P_\Sigma}}{d} \tag{3}$$

Electric field strength in units of dBμV/m, expressed in dB

$$E_0 = 74.77 + 10\lg P_\Sigma - 20\lg d \tag{4}$$

3. Pantograph Disconnection Discharge Model
3.1. Simulation Software

FEKO means field calculation of arbitrary shape [10-13]. FEKO's core algorithm is the method of moments (Mom). For metallic conductor or dielectric, first calculate the surface current distribution, thus you can calculate the RCS pattern of near-field and far-field or the input impedance of antenna. As for electrically large objects, you can use physical optics method (PO) and uniform geometrical theory of diffraction (UTD) solution [14-16]. FEKO make use of mixing method of Mom / PO and Mom / UTD to solve ensure accuracy of electrically large problems.

Method of moments based on the principle of superposition, the purpose is to solve linear equations. Assuming that the given boundary value field equation is expressed as follows unified operator equation

$$L(f) = g \tag{5}$$

Where, L represents a linear operator; f is the unknown function; g for activation function. Using the moment method of solving equations (5) is to expand the f with known function $\{ f_n \}$ in the operator definition domain

$$f = \sum_{n=1}^{\infty} I_n f_n \tag{6}$$

Where, I_n is the unknown coefficients, f_n as basis functions.

Take the above equation finite terms into formula (5), the equation will be approximately equal close on both sides

$$L\left[\sum_{n=1}^{N} I_n f_n(r')\right] \approx g(r) \tag{7}$$

I_n must be determined a finite number in order to make the best possible approximation approximate exact solution. Thus defined residual $R(r)$

$$R(r) = L\left[\sum_{n=1}^{N} I_n f_n(r')\right] - g(r) \tag{8}$$

It is the exact solution *when R(r)= 0*, but generally lack of exact solutions, so make $R(r)$ as small as possible. So choose a known function $\{W_m\}$ as a weighting function, so that the inner product of residual $R(r)$ and all $\{W_m\}$ is zero

$$\langle W_m(r) \quad R(r)\rangle = 0 \qquad m = 1, 2, 3, \cdots N \tag{9}$$

Inner product also known as the demand moments, so called method of moments . Thus leading with N unknowns I_n linear equations

$$\sum_{n=1}^{N} I_n \langle W_m, L(f_n)\rangle = \langle W_m, g\rangle \qquad m = 1, 2, 3, \cdots N \tag{10}$$

Expressed as a matrix equation

$$[Z] \ [I] = [V] \tag{11}$$

Where, [Z] is a $N \times N$ square matrix, called the generalized impedance matrix, obtained [I] by solving the above equation, you can get the approximate solution of equation (5).

3.2. Electric Locomotive Spark Model
In order to better simulate the actual situation of pantograph system, when creating a model in CADFEKO we take into account the effect of contact line, catenaries, dropper, pantograph, and bodywork. Catenaries system model as shown in Figure 1, Z axis represents the forward, that is the direction perpendicular to the ground and in the pantograph slider center, X axis represents the longitudinal direction, i.e. the train running direction, Y axis represents the transverse direction to the lateral field.
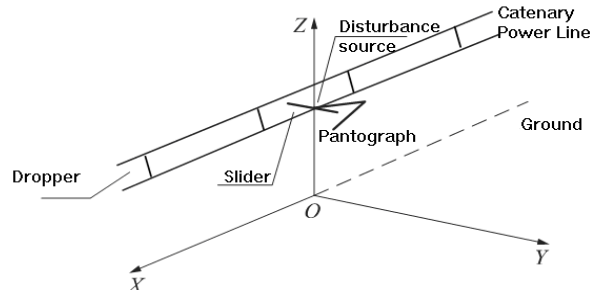
Figure 1. Catenaries system model

The model consists of catenaries body and earth body, choose length 25.5 m, width 3.5 m, height 3.7 m alloy aluminum car, thickness of the aluminum d=5×10^{-3}m, conductivity σ=

3.54×10^7 s/m ,inside vehicle is the free space , distance from vehicle body to ground is0.6 m. Catenaries length is 300 m, wire radius select 6.18×10^{-3} m, conductivity σ=5.15×10^7 s/m, relative permittivity ε_r= 0,ground conductivity σ=5×10^{-3} s/m, relative permittivity ε_r = 10, between the soil and gravel. The interference voltage source select 100V, location coordinates (0,0,6). Modeling options for pantograph select pure carbon material, length of 1.9m.

In order to better simulate the actual condition of trains, trains model added eight windows, the size is 1.35 m ×0.65 m, then simulation results for different frequencies are shown in Figure 2 to 9.

3.3. Simulation Results
Figure 2 is simulation result based on catenaries system model with CADFEKO software, then crosscutting the model with PREFEKO process, we get the transverse near-field map when frequency is 10 MHz, the diagram distinguish radiation field intensity according to different colors. It can be clearly observed that, due to the shielding effect of trunk metal material, the electric field strength within passage is very low, almost close to zero, but does not achieve complete shielding of electromagnetic radiation for reasons of windows.
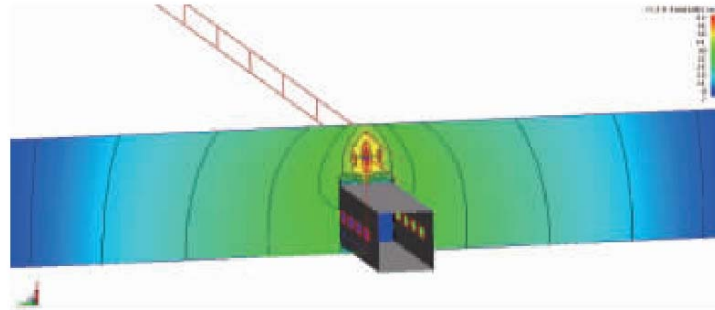
Figure 2. Transverse near-field map of 10 MHz

Electric field strength at different distances of EMU window glass inside is statistically significantly ($P <0.05$). Comparisons with other points, electric field intensity at 0 cm from glass is highest ($P <0.05$); panning off glass toward to middle of compartment, electric field strength is decreasing, electric field strength at sidewall 0 cm is basically the same as other parts of body. Seen in Table 1.

Table 1. Electric field intensity at glass inside of EMU and wall inside (n = 21, x ± s, kV / m)

Type	glass inside 0 cm	glass inside 10 cm	glass inside 20 cm	wall inside 0 cm
CRH2	0.025±0.008[a]	0.015±0.001	0.011±0.002	0.011±0.001
CRH5	0.022±0.006[a]	0.017±0.003	0.011±0.003	0.011±0.002

Note: a comparison with other measuring points ＜0.05。

When EMU is running, electric field strength of Type CRH2 at the bottom of motor and under pantograph is statistically significant ($P <0.05$), thus electric field inside the motor is higher; For Type CRH5 electric field intensity at bottom of motor and the under pantograph is not so significant. Which can be seen in Table 2?

Table 2. Electric field strength at position motor inside and carriage under pantograph (x ± s, kV / m)

Type	Monitoring Points	position motor inside	carriage under pantograph
CRH2	28	0.024±0.013[a]	0.011±0.002
CRH5	35	0.018±0.011	0.011±0.001

Notes: a comparison with carriage under pantograph, $P <0.05$.

See in Table 3, electric field strength at vertical distance 0 m and 1.5 m is statistically significant (P <0.05), whereas electric field intensity from vertical 1.5 m the is higher.

Table 3. Electric field strength at parallel different points of station（n=3，x±s，kV/m）

vertical distance 0 m	1 m	1.1~2 m	2.1~3 m
0	0.036±0.005	0.032±0.042	0.025±0.032
1.5	1.810±0.450[a]	1.816±0.059[a]	1.416±0.430[a]

Notes: a comparison with vertical distance 0 m，P＜0.05.

Figure 3.a and Figure 3.b show the electromagnetic interference caused by pantograph, concerned horizontal 20m away, when the simulation frequency is of 10, 20 and 30MHz respectively, within lateral distance 20 ~ 70m, transverse attenuation is of 8,13 and 17 dB, nevertheless the lateral decay has reached more than 10 dB when frequency is of 100, 200, 300 MHz. The peak of pantograph electromagnetic radiation primarily depends on power dissipation, simulation carried out 100W and 200W experiments, when total power is set to 200W, its radiation peak is significantly higher than the former.
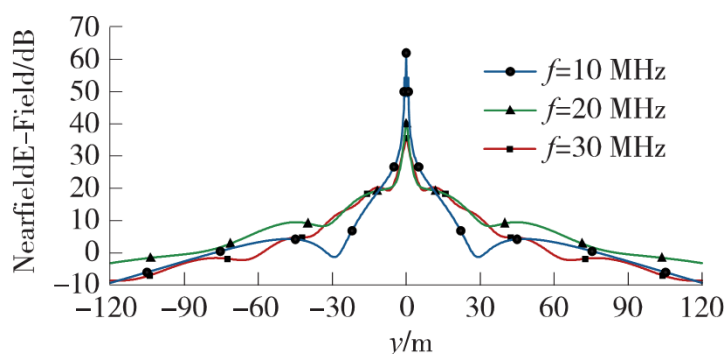
Figure 3.a. Transverse attenuation curve of 10, 20, 30 MHz
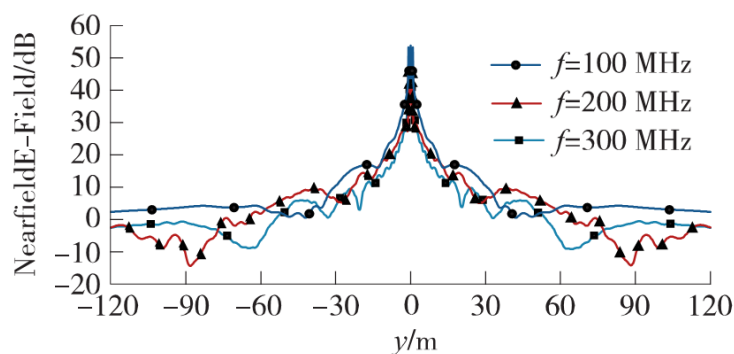
Figure 3.b. Transverse attenuation curve of 100,200,300 MHz

Figure 4.a and Figure 4.b show forward direction (i.e. Z axis) attenuation curve under different frequencies. As we focus on the field intensity distribution 50 m above the pantograph, it can be seen that within range of 8 ~ 38m, electric field attenuation reaches about 10 dB. When the frequency below 20 MHz, attenuation of electric field strength inside almost reaches 80 dB; when the frequency greater than 30 MHz, the bodywork can not play a good shielding effect, the attenuation of field strength inside reaches 40 dB.
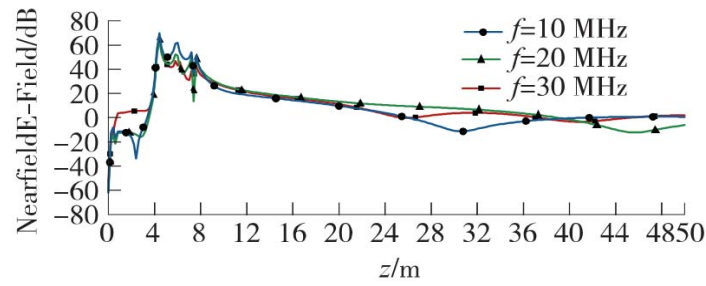
Figure 4.a. Forward attenuation curve of 10,20,30 MHz
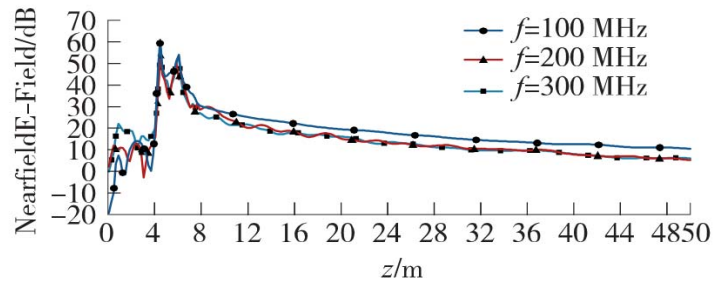
Figure 4.b. Forward attenuation curve of 100,200,300 MHz

Figure 5.a and Figure 5.b show the longitudinal electric field distribution of contact line under different frequencies, for comparison, we chose different locations when Z = 6 m. It is obvious that when frequency is 10 MHz and distance 50 m , the decay rate is greater than under 20 MHz electromagnetic wave. When frequency is of 100 ~ 200 MHz, they decay faster. Here can get a common rule, at the beginning decay very quickly, after a certain distance has gradually slowing trend. The reason is electromagnetic energy propagation in the space medium, catenaries as a guided wave system plays the role of directing electromagnetic energy flow.
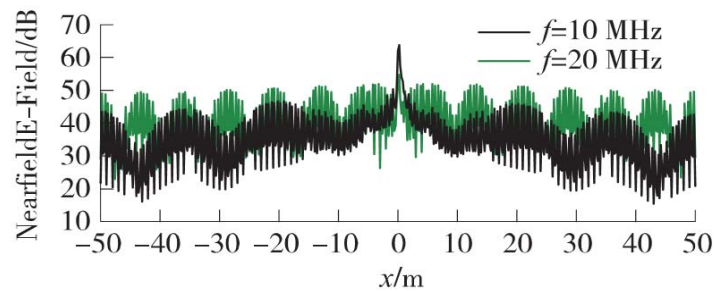
Figure 5.a. Longitudinal attenuation curve of 10,20 MHz
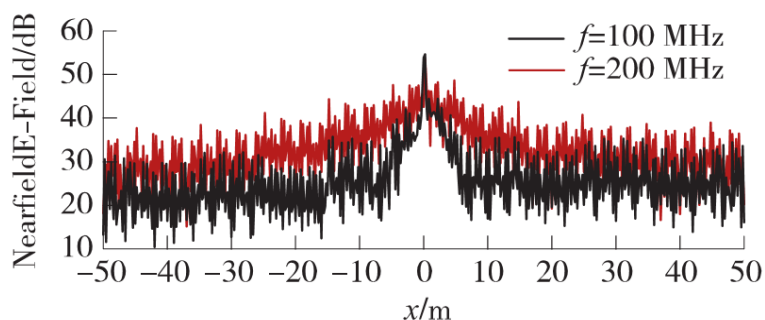
Figure 5.b. longitudinal attenuation curve of 100,200 MHz

In the simulation we pay particular attention to the far-field gain when below frequency of 30MHz, φ = 0 °. As shown in Figure 6, the presence of pantograph, results in the asymmetry of its diagram.
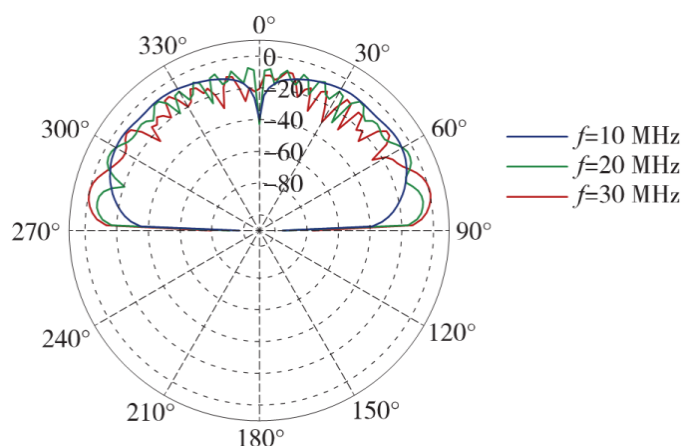
Figure 6. Far-field gain of 10,20,30 MHz

4. Conclusion

Pantograph can be seen as an antenna, the radiated no longer returned power is dissipated power, called radiated power. The electromagnetic radiation value generated by pantograph, depends on the radiation power and its position. Our main concern is the electromagnetic pollution levels on both sides of railway, i.e. the electromagnetic interference degree within scope of 20 m away from rail, 3. 5 m above the ground, it can be seen in the simulation, in this range when line voltage is 100 V, electric field attenuation to 0 dB or so. Additionally, within range of forward (Z axis) distance 50 m, the electromagnetic wave below 30 MHz decay faster than above 100 MHz ,and outside 40 m, it reduced to less than 0 dB, this has a certain reference value to reduce radiated noise effects on 3 ~ 30 MHz shortwave transmitter antenna along electrified railway field.

Through simulation experiments, the electromagnetic waves attenuation characteristics generated by pantograph, has some reference value on how to measure high-speed railway electromagnetic interference and electromagnetic compatibility assessment. With the rapid development of high-speed railway, the railway EMC standards re-revision is inevitable trend. However, due to complexity of high-speed railway environment, measurements on the spot has great difficulties, Using computer simulation can make up for this shortfall to some extent. Foreign high-speed electrified railway development has experienced a long history, the development of electromagnetic compatibility standards, in addition to from abroad, new standard should be adapt to China's high-speed railway features.

Acknowledgment

References

[1] N Hanigovszki, J Landkildehus, G Spiazzi, F Blaabjerg. An EMC Evaluation of the Use of Unshielded Motor Cables in AC Adjustable Speed Drive Applications. *IEEE Trans. Power Electron*. 2006; 21(1, 1): 273–281.

[2] YH Wang. Analysis of very high frequency electromagnetic interference to Coal Mine distribution. *Telecommunications Science*. 2002; (3).

[3] Meng Jin, Ma Weiming etc. *High Frequency Model of Conducted EMI for PWM Variable-speed Drive Systems*. Proceedings of the CSEE. 2008; 5: 141–143.

[4] LF Cheng, JP Sun. Influence of electrical parameters on electromagnetic waves propagation in rectangular tunnels. *Chinese Journal of Radio Science*. 2007; (3).

[5] H Akagi, T Doumoto. A passive EMI Filter for Preventing High-Frequency Leakage Current from Flowing through the Grounded Inverter Heat Sink of an Adjustable-Speed Motor Drive System. *IEEE Transactions on Industry Applications*. 2005; 41(5, 9): 1215–1223.

[6] WF Li, YL Lv. Experiment on characteristic of radio propagation in mine. *Journal of Xi'an University of Science and Technology*. 2008; (2).

[7] GAO Zong-bao, WU Guang-ning, LU Wei, Etc. Research Review of Arc Phenomenon between Pantograph and Catenary in High-speed Electrified Railway. *High Voltage Apparatus*. 2009; 45(3): 104-108.

[8] CHEN Song, SHA Fei, WANG Guo-dong. Modeling and Simulating Impulse RF Noises of Electrical Railways in Simulink Environment. *Journal of China Railway Society*. 2009; 31(1): 55- 58.

[9] HQ Zhang, HZ Yu. Multipath Transmission Modeling and Simulating of Electromagnetic Wave In Rectangle Tunnel. *Chinese Journal of Radio Science*. 2008; (1).

[10] HAN Tong-xin.Reason Analysis for Continuous Spark in Current Collection of Catenary-pantograph System. *Railway Locomotive & CAR*. 2003; 23(3) 58- 61.

[11] Wang Ling-chao. Exploration on Electro-magnetic Compatibility and the Standards of Railway Technical Equipment. *Railway Quality Control*. 2009; 37(5): 3-4.

[12] Wu Ji-qin. Occurrence of Arc in Pantograph and Overhead Contact System and Its Interference. *Electric Railway*. 2008; (2): 27-29.

[13] Meng Jin, Ma Weiming. Power converter EMI analysis including IGBT nonlinear switching transient model. *IEEE Trans. on Industrial Electronics*. 2006; 54(5): 1577–1583.

[14] F Costa, C Vollaire, R Meuret. Modeling of Conducted Common Mode Perturbations in Variable-Speed Drive Systems. *IEEE Transactions on Electromagnetic Compatibility*. 2005; 14(4, 11): 1012–1021.

[15] YP Zhang, WM Zhang. Characterization of UHF radio propagation channels in a long wall face of a coal mine. *Journal of China Coal Society*. 2000; (4).

[16] YC Son and SK Sul. Conducted EMI in PWM inverter for house-hold electric appliance. *IEEE Trans. Power Electron*. 2002; 38(5, 9): 1370–1379.